ELSEVIER

Nuclear Instruments and Methods in Physics Research A 465 (2001) 60–69

NUCLEAR INSTRUMENTS & METHODS IN PHYSICS RESEARCH Section A

www.elsevier.nl/locate/nima

Developments for radiation hard silicon detectors by defect engineering—results by the CERN RD48 (ROSE) Collaboration☆

G. Lindström[a,*], M. Ahmed[b], S. Albergo[c], P. Allport[d], D. Anderson[e], L. Andricek[f], M.M. Angarano[g], V. Augelli[h], N. Bacchetta[i], P. Bartalini[g], R. Bates[i], U. Biggeri[k], G.M. Bilei[g], D. Bisello[j], D. Boemi[c], E. Borchi[k], T. Botila[l], T.J. Brodbeck[m], M. Bruzzi[k], T. Budzynski[n], P. Burger[o], F. Campabadal[p,q], G. Casse[d], E. Catacchini[k], A. Chilingarov[m], P. Ciampolini[g], V. Cindro[r], M.J. Costa[p,q], D. Creanza[h], P. Clauws[s], C. Da Via[b], G. Davies[t], W. De Boer[u], R. Dell'Orso[v], M. De Palma[h], B. Dezillie[w], V. Eremin[x], O. Evrard[o], G. Fallica[y], G. Fanourakis[z], H. Feick[aa], E. Focardi[k], L. Fonseca[p,q], E. Fretwurst[a], J. Fuster[p,q], K. Gabathuler[ab], M. Glaser[ac], P. Grabiec[n], E. Grigoriev[u], G. Hall[ad], M. Hanlon[d], F. Hauler[u], S. Heising[u], A. Holmes-Siedle[b], R. Horisberger[ab], G. Hughes[m], M. Huhtinen[ac], I. Ilyashenko[x], A. Ivanov[x], B.K. Jones[m], L. Jungermann[u], A. Kaminsky[i], Z. Kohout[ae], G. Kramberger[r], M. Kuhnke[a], S. Kwan[e], F. Lemeilleur[ac], C. Leroy[ar], M. Letheren[ac], Z. Li[w], T. Ligonzo[h], V. Linhart[ae], P. Litovchenko[ag], D. Loukas[z], M. Lozano[p,q], Z. Luczynski[ah], G. Lutz[f], B. MacEvoy[ad], S. Manolopoulos[j], A. Markou[z], C. Martinez[p,q], A. Messineo[v], M. Miku[r], M. Moll[ac], E. Nossarzewska[ah], G. Ottaviani[ai], V. Oshea[j], G. Parrini[k], D. Passeri[g], D. Petre[l], A. Pickford[j], I. Pintilie[l], L. Pintilie[l], S. Pospisil[ae], R. Potenza[c], V. Radicci[h], C. Raine[j], J.M. Rafi[p,q], P.N. Ratoff[m], R.H. Richter[f], P. Riedler[ac], S. Roe[ac], P. Roy[af], A. Ruzin[aj], A.I. Ryazanov[ak], A. Santocchia[ad], L. Schiavulli[h], P. Sicho[al], I. Siotis[z], T. Sloan[m], W. Slysz[n], K. Smith[j], M. Solanky[b], B. Sopko[ae], K. Stolze[am], B. Sundby Avset[an], B. Svensson[ao], C. Tivarus[l], G. Tonelli[v], A. Tricomi[c], S. Tzamarias[z], G. Valvo[y], A. Vasilescu[ap], A. Vayaki[z], E. Verbitskaya[x], P. Verdini[v], V. Vrba[al], S. Watts[b], E.R. Weber[aa], M. Wegrzecki[n], I. Wegrzecka[n], P. Weilhammer[ac], R. Wheadon[v], C. Wilburn[aq], I. Wilhelm[ar], R. Wunstorf[as], J. Wüstenfeld[as], J. Wyss[i], K. Zankel[ac], P. Zabierowski[ah], D. Zontar[q]

☆Presented at the LEB workshop Cracow, September 2000, see CERN report CERN 2000-010 CERN/LHCC/2000-041.

*Corresponding author. Tel.: +49-40-8998-2951; fax: +49-40-8998-2959.

E-mail address: gunnar@sesam.desy.de (G. Lindström).

0168-9002/01/$ - see front matter
PII: S0168-9002(01)00347-3

[a] University of Hamburg, II Institut fur Experimentalphysik, Gbd. 67b, Luruper Chaussee 149, 22761 Hamburg, Germany
[b] Brunel University, London, UK
[c] Catania University, Catania, Italy
[d] University of Liverpool, Liverpool, UK
[e] Fermilab, Batavia, IL, USA
[f] Max Planck Institute, Munich, Germany
[g] University of Perugia, Perugia, Italy
[h] Dipartimento Interateneo di Fisica and INFN, Bari, Italy
[i] Padova University and INFN, Italy
[j] Glasgow University, UK
[k] Firenze University, Florence, Italy
[l] Institute of Physics and Technology of Materials, Bucharest, Romania
[m] Lancaster University, UK
[n] Institute of Electron Technology (ITE), Warsaw, Poland
[o] Canberra Semiconductor N.V., Belgium
[p] Centro Nacional de Microelectronica, Barcelona, Spain
[q] Instituto de Fisica Corpuscular, Valencia, Spain
[r] Jožef Stefan Institute and Department of Physics, University of Ljubljana, Ljubljana, Slovenia
[s] Gent University, Belgium
[t] Kings College, London, UK
[u] Karlsruhe University, Karlsruhe, Germany
[v] Pisa, INFN, Italy
[w] Brookhaven National Laboratory, Upton, NY, USA
[x] Ioffe Physico-Technical Institute, St. Petersburg, Russia
[y] STMicroelectronics, Catania, Italy
[z] Institute of Nuclear Physics, Demokritos, Greece
[aa] Department of Materials Science and Engineering, University of California, Berkeley, CA, USA
[ab] PSI, Villigen, Switzerland
[ac] CERN, Geneva, Switzerland
[ad] Imperial College, London, UK
[ae] Czech Technical University, Prague, Czech Republic
[af] Montreal University, Montreal, Canada
[ag] Institute for Nuclear Research, Academy of Sciences, Kiev, Ukraine
[ah] Institute of Electronic Materials Technology (ITME), Warsaw, Poland
[ai] Modena University, Italy
[aj] Department of Engineering, Tel Aviv University, Tel Aviv, Israel
[ak] Kurchatov Institute, Moscow, Russia
[al] Institute of Physics, Academy of Sciences, Prague, Czech Republic
[am] CiS Institut für Mikrosensorik gGmbH, Erfurt, Germany
[an] SINTEF, Oslo, Norway
[ao] Royal Institute of Technology, Stockholm, Sweden
[ap] Institute of Nuclear Physics and Engineering, Bucharest, Romania
[aq] Micron Semiconductor Ltd., Lancing, UK
[ar] Faculty of Mathematics, and Physics, Institute of Particle and Nuclear Physics, Charles University, Prague, Czech Republic
[as] Dortmund University, Dortmund, Germany

Received 16 November 2000; accepted 19 November 2000

Abstract

This report summarises the final results obtained by the RD48 collaboration. The emphasis is on the more practical aspects directly relevant for LHC applications. The report is based on the comprehensive survey given in the 1999 status report (RD48 3rd Status Report, CERN/LHCC 2000-009, December 1999), a recent conference report (Lindström et al. (RD48), and some latest experimental results. Additional data have been reported in the last ROSE workshop (5th ROSE workshop, CERN, CERN/LEB 2000-005). A compilation of all RD48 internal reports and a full publication list can be found on the RD48 homepage (http://cern.ch/RD48/). The success of the oxygen enrichment of

FZ-silicon as a highly powerful defect engineering technique and its optimisation with various commercial manufacturers are reported. The focus is on the changes of the effective doping concentration (depletion voltage). The RD48 model for the dependence of radiation effects on fluence, temperature and operational time is verified; projections to operational scenarios for main LHC experiments demonstrate vital benefits. Progress in the microscopic understanding of damage effects as well as the application of defect kinetics models and device modelling for the prediction of the macroscopic behaviour has also been achieved but will not be covered in detail.

PACS: 29.40.Wk; 85.40.Ry; 61.82.Fk; 72.20.Ju

Keywords: Silicon detectors; Gamma-, neutron-, proton- and pion irradiation; Improved radiation tolerance by oxygen enrichment; Annealing studies; Consequences for high energy physics applications

1. Defect engineered silicon

The key idea of the RD48 strategy had been to improve the radiation tolerance of silicon by defect engineering, involving the deliberate addition of impurities to the bulk material in order to affect the damage induced formation of electrically active defects and thus control macroscopic device parameters. As it is well known that oxygen and carbon are capturing the primary radiation induced vacancies and interstitials in the silicon lattice these impurities were singled out as most promising for an improved radiation tolerance.

Various types of silicon had been investigated in the past, covering most of the accessible phase space as to both impurities. In contrast to carbon a considerably increased oxygen content proved to be highly beneficial. Hence the efforts had concentrated on that and finally, based on earlier experiments at BNL [5], a method had been adopted consisting of a high temperature diffusion of oxygen through the silicon bulk, using the silicon-oxide layer as supply source. In the following this method will be referred to as Diffusion Oxygenated Float Zone silicon (DOFZ).

Oxygen depth profiles obtained by different diffusion scenarios are displayed in Fig. 1, as measured by SIMS [6]. The DOFZ technology proved to be feasible and cost effective, as it can be readily incorporated in the normal manufacturing process. The basic technical development had been performed by ITE [7]. It was meanwhile successfully transferred to possible Si-detector vendors for LHC (SINTEF, CiS, STMicroelectronics and Micron [8–11]). All these companies are members of the RD48 collaboration. More details of the DOFZ method may be found in Ref. [1].

2. The oxygen effect

The following three main macroscopic effects are seen in silicon detectors after energetic hadron irradiation:

- Change of the doping concentration with severe consequences for the needed operating voltage.
- Fluence proportional increase in the leakage current, caused by the creation of recombination/generation centres.
- Deterioration of charge collection efficiency due to charge carrier trapping with impact on the signal height produced by mip's.

The volume generated current has been shown to be of universal nature, both as to the absolute value and annealing properties as function of time after irradiation. If normalised to the sensitive

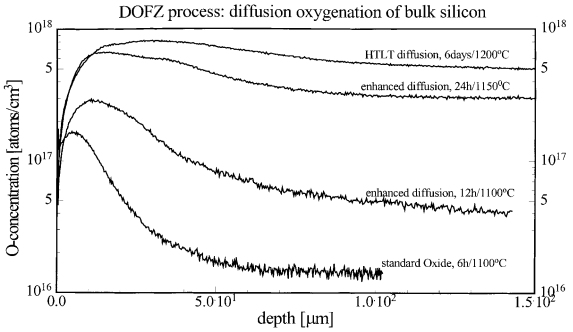

Fig. 1. Oxygen depth profile as measured by SIMS.

volume and to the 1 MeV-neutron equivalent hadron fluence, the effect is independent of any material property and manufacturing process used [12,13]. However cooling to an operating temperature of about –10°C guarantees a sufficiently low noise and dissipation power [14]. The trapping effect looks also to be tolerable for ensuring the needed S/N ratio for mip's [15]. The first effect is the most severe, as the operating voltage cannot be increased to very high levels. The beneficial effect of oxygenation is clearly displayed in Fig. 2. Here we have measured the combined effect of successive irradiation and constant annealing steps in between (4 min at 80°C), which resemble the yearly room temperature warm up periods during maintenance in LHC experiments. Starting from the original n-type material the effective donor concentration is reduced in the lower fluence range, whereas the increasing generation of acceptor like defects leads eventually to type inversion and an almost linear increase thereafter. The measurements show clearly that the slope of that increase depends largely on the oxygen and carbon concentration. There is a factor of 3 gain in radiation hardness by high [O] whereas high [C] leads to a worsening with respect to standard silicon.

Unfortunately, the gained improvement is only visible after charged hadron irradiation (independent whether produced by protons or pions) whereas for neutron induced damage the DOFZ-effect leads only to benefits in connection with low resistivity silicon [16].

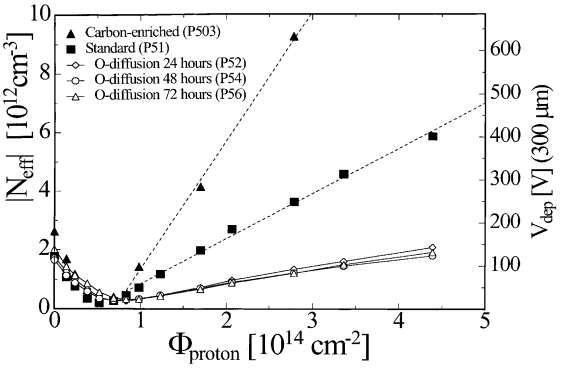

Fig. 2. Influence of carbon and oxygen on V_{dep}.

It should be emphasised that the oxygenation technique does not have any adverse effect as to the normal detector behaviour both regarding the bulk (diode characteristic) and the surface related properties [17,18].

3. Modelling of damage effects in N_{eff}

The measurements referred to in the previous section have proved to be extremely useful in surveying different material as to their respective radiation tolerance. However, these tests reveal only one of the relevant parameters in the change of N_{eff} (resp. the depletion voltage) namely the behaviour at or around the minimum of the annealing function. For a full modelling of what will be expected during operational scenarios in the 10 years LHC period, one has to measure the combined effect of damage and its subsequent annealing in more detail. Such an approach had been taken by several groups [19–21]. The experiments are performed using a full set of test diodes irradiated at room temperature with different fluences. Annealing experiments are carried out at constant elevated temperature (e.g. $+60^0$C or 80^0C) in order to accelerate the effect of long term annealing and thus compress the 10 years effect at LHC into a time span of only weeks.

The principal components seen by such measurements are shown in Fig. 3. With $\Delta N_{eff} = N_{eff,0} - N_{eff}(\Phi, t, T)$ being the change between the initial

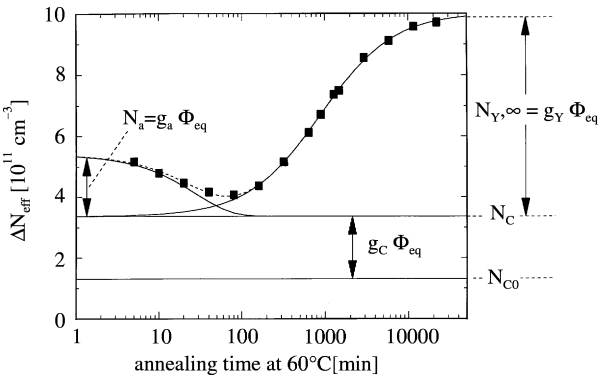

Fig. 3. Different components of the N_{eff} annealing as parameterised by the Hamburg model: $\Delta N_{eff} = N_a(\Phi, t(T)) + N_C(\Phi) + N_Y(\Phi, t(T))$.

doping concentration of the base material and its value after irradiation with fluence Φ and after annealing during t at temperature T, one can readily decompose the complex function into a short term annealing N_a with time constant τ_a, a time independent term N_C (stable acceptor generation) and a long term or "reverse" annealing N_Y with time constant τ_Y. It should be noted that only the time constants are depending on the annealing temperature whereas the amplitudes are only functions of the fluence. The analysis of all three components as function of annealing temperature, annealing time and fluence had then led to a description which is referred to as the "Hamburg model" [19]. In Fig. 4 examples are given for such annealing curves after proton irradiation up to 1×10^{15} p/cm^2. The fits to the data are excellent and thus the parameters extracted both for standard (non-oxygenated) and DOFZ (oxygenated) silicon diodes are trusted to be reliable (see Fig. 5). As was already obvious from Fig. 2, the slope for the constant acceptor generation g_C is improved by more than a factor of 3 using O-rich instead of standard silicon. Fig. 6 shows an additional and completely unexpected beneficial effect, as the amplitude for reverse annealing is not anymore increasing proportionally to the fluence but strongly saturating. It is important to notice that the temperature dependence is governed by a single activation energy leading to an almost complete freezing of the reverse annealing during the operational period [22]. The reverse annealing becomes, however, relevant during the annual maintenance periods at room temperature. The saturating and delay (Fig. 6 left and right, respectively) for O-rich silicon offers therefore a substantial safety margin.

Using the parameters extracted from annealing experiments with standard and O-rich silicon, the Hamburg model had then been used for projections to full 10 years LHC scenarios. Fig. 7 gives an example for the ATLAS pixel detector: B-layer, located at a radial distance of 4 cm and being subjected to a total annual fluence of 3.5×10^{14} cm^{-2} (1 MeV neutron equivalent, consisting of 85% charged hadrons). For standard material the depletion voltage is surpassing the tolerated operational voltage already after the third LHC year whereas for the O-rich silicon the pixel sensor may be really operable during the whole LHC period. The difference between standard and DOFZ silicon becomes even more pronounced if one would have to increase the length of the maintenance period from the foreseen scenario (3 days 20°C and 2 weeks 17°C) to larger times and higher temperatures.

Additional experiments had been performed, which confirm the results given above (e.g. by the BNL group [21], and include also irradiation under bias and at low temperature (JSI-Ljubljana [20]).

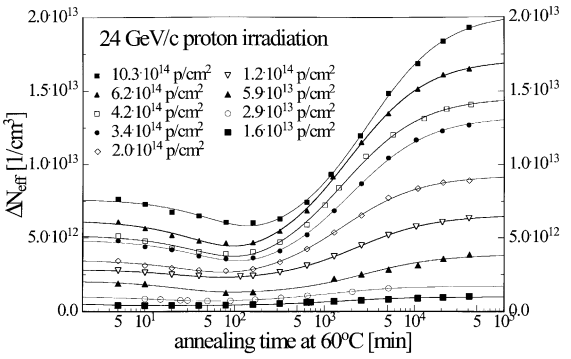

Fig. 4. Systematic measurements of N_{eff}-annealing in DOFZ silicon diodes after 24 GeV/c-proton irradiation.

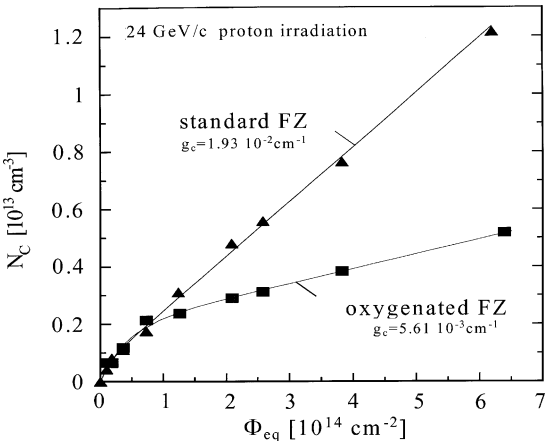

Fig. 5. Stable damage generation as observed in standard and DOFZ silicon diodes.

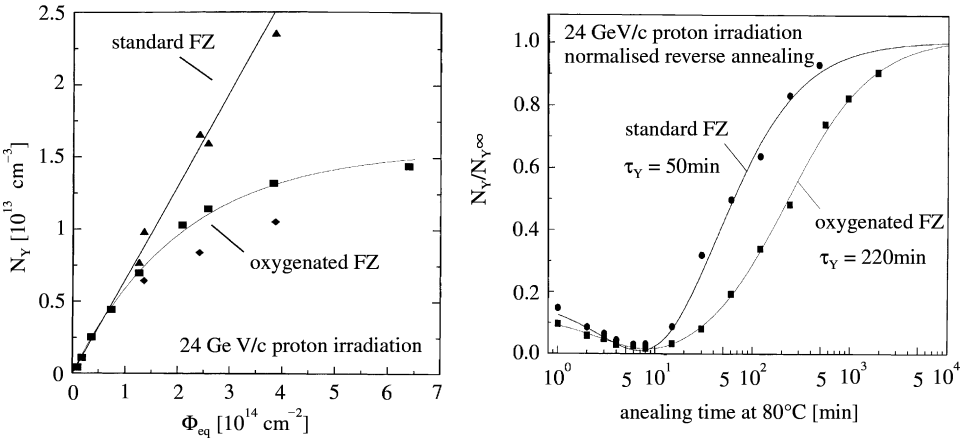

Fig. 6. Amplitude (left) and time constant (right) of reverse annealing measured with standard and DOFZ silicon diodes.

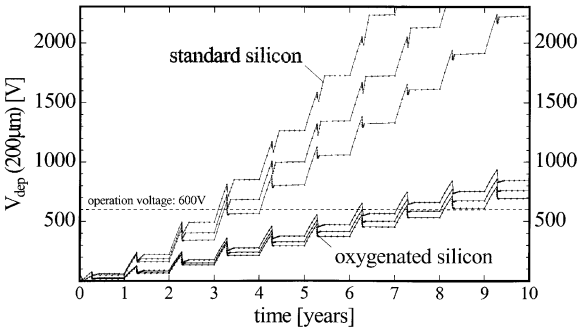

Fig. 7. Damage projections for the ATLAS pixel B-layer for different LHC scenarios beam period 100 days at –7°C maintenance (from bottom to top curve): (1) 3 d at 20°C + 14 d at 17°C, (2) 30 d at 20°C; (3) 60 d at 20°C.

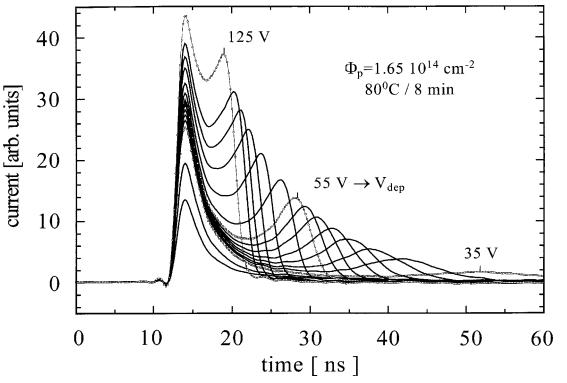

Fig. 8. Time resolved current pulses generated by illumination with nsec IR laser pulses after damage with 1.65×10^{14} p/cm^2, measured after 8 min annealing at 80°C.

4. A closer look: charge collection and depletion voltage

It has often been argued that the results described in Section 3 are primarily based on the measurements of the depletion voltage using capacitance/voltage characteristics, while what is really relevant for the LHC experiments is the necessary operating voltage to ensure good S/N ratio for mip's. In a number of experiments we have therefore compared the results obtained from C/V measurements with those done by charge collection, illuminating the diode either with ultrashort infrared laser pulses or performing experiments with minimum ionising electrons from a beta source [15,23–27].

As an example, Fig. 8 shows the time-resolved current pulses as function of bias voltage for an annealing step equivalent to a 4 weeks maintenance period at RT [28]. The double peaking seen most pronouncedly after such short annealing time is well known and documents that the detector can no longer be regarded as an asymmetric junction but rather displays junctions at both the front and the rear side. Correspondingly, electric fields penetrate into the bulk material upon reverse biasing from both sides. For larger annealing times this behaviour disappears. The accumulated charge within a certain time window can be plotted as function of the bias voltage enabling an independent way of extracting the

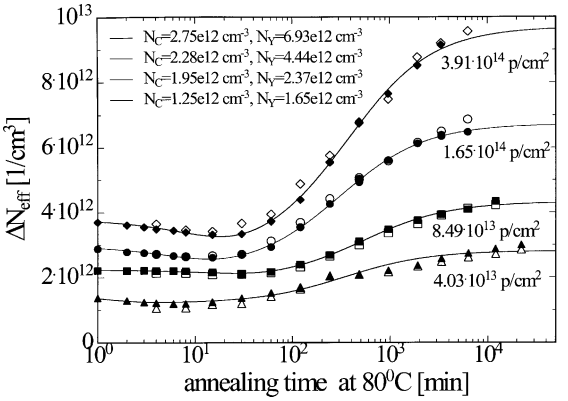

Fig. 9. Annealing curves as measured from charge collection (open symbols) and capacitance/voltage characteristics.

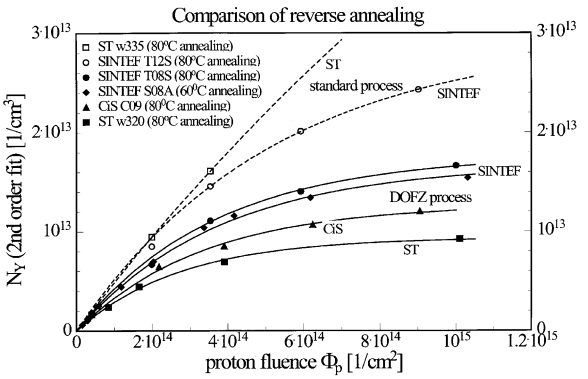

Fig. 10. Reverse annealing for diodes from different manufacturers; comparison of standard and DOFZ process.

depletion voltage. The comparison of both CCE/V (charge collection efficiency vs. voltage) and C/V (capacitance vs. voltage) results is given in Fig. 9 revealing an excellent correspondence of both methods. However due primarily to trapping effects the operating voltage should always be larger than the depletion voltage. The necessary overbias depends on the fluence and state of annealing, but as rough estimate a 100 V safety margin should be added [29].

5. Transfer of DOFZ to manufacturers

As pointed out above, the DOFZ technology had meanwhile been transferred to several manufacturing companies. In this section, examples are given for samples from SINTEF, CiS and STMicroelectronics [8–10]. Fig. 10 shows a survey of results for the reverse annealing effect and its correlation to SIMS measurements on the same wafers [30]. If measured in the full fluence range up to 1×10^{15} p/cm^2 the decrease of N_Y/Φ for O-rich compared to standard material becomes even more pronounced. A saturation value for the most O-rich sample from STMicroelectronics of 9×10^{12} cm^{-3}, amounting to only 250 V increase of depletion bias for a 200 μm thick pixel detector, is reached. This is even much better than assumed for the simulation shown in Fig. 7 and thus improve the lifetime of these components above present expectations.

Due to the differences in the individual processes for the O-enrichment used by the involved companies there is a certain variance in this saturation value, but compared to the different average O-concentrations displayed in Fig. 11, the scatter is surprisingly small. An optimum could very well be in the order of a 24 h diffusion at 1150°C, which can be readily performed by all companies. It is also evident from the comparison of Figs. 10 and 11 that even the standard process leads to individual differences in the oxygen depth profile. While the lowest O-concentration (ST-process) leads to an almost linear dependence of N_Y on fluence, the substantially higher O-values in the SINTEF standard process shows already some saturation at higher fluences. It cannot be ruled out that the inhomogeneous oxygen concentration in the silicon bulk and its dependence on the individual process is partly responsible for the variance seen in the radiation hardness of diodes manufactured using a standard process and it could also be partly responsible for the double junction effect. It should be emphasised that the results obtained here with DOFZ produced diodes have meanwhile been confirmed by test experiments with ATLAS strip and pixel detectors [14,31]. We have also verified, that these results

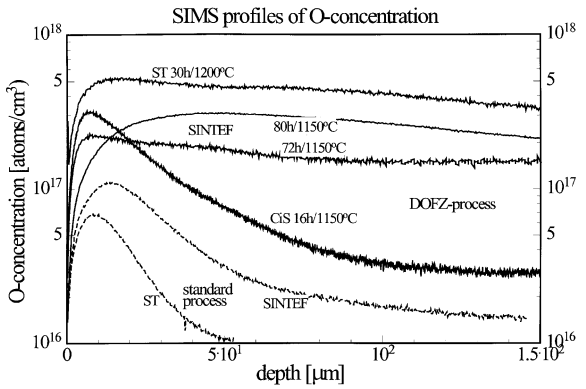

Fig. 11. Depth profiles of oxygen concentration measured by SIMS for diodes used in the experiments of Fig. 10 (see text).

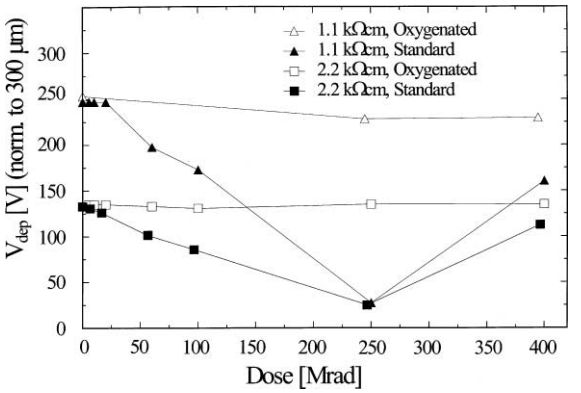

Fig. 12. Effects of γ-irradiation in standard and DOFZ silicon diodes: constant V_{dep} up to 400 Mrad for O-rich Si.

are fully reproduced in damage studies with pion irradiation [30].

6. A brief look on the N–P-puzzle

The collaboration had done extensive investigations on the details of defect formation and kinetics during annealing, see the last status report and publications cited there [1]. One point illuminating the effect of O-enrichment and the differences seen between neutron and charged hadron irradiation is worth mentioning here. Note that this difference is present after proper NIEL scaling and hence in contradiction to the widely used assumption that all bulk damage is strictly proportional to the non-ionising energy loss. Due to this contradiction we refer to it often as the n–p-puzzle.

On a microscopic scale the damage produced by energetic hadron irradiation is composed of the generation of isolated point defects and a dense accumulation of displacements generated at the end of primary recoil ranges, usually referred to as defect clusters. The main difference between MeV neutron damage and that produced by energetic protons or pions is then, that the total NIEL in n-damage is governed predominantly by the production of clusters, due to the average energetic recoil energies in the primary hadronic interactions, whereas for charged particles the additional Coulomb interaction leads to quite low energy recoils. These are more likely to produce point defects. In fact this notion had been verified by experiments (see [32]) and detailed simulations are under way [33]. Present defect models attribute the O-effect especially to the point defects. Hence the observed radiation hardening effect present in charged particle damage but almost absent after neutron damage can be understood.

This is nicely confirmed by results from gamma irradiation, undertaken at BNL [34]. In this case the displacement damage in the detector bulk is entirely due to Coulomb interaction of electrons with silicon nuclei. The average recoil energies are extremely low and thus the damage is almost entirely due to point defects. Hence the O-enrichment has an even larger effect than for hadron irradiation (see Fig. 12). For O-enriched diodes, irrespective of the initial doping concentration the depletion voltage stays practically constant over a wide dose range whereas for standard devices one gets type inversion similar as seen in hadron irradiation.

Although a lot is needed to understand the damage effects in the macroscopic detector behaviour on the basis of the microscopic results in a fully quantitative way, it is fair to say, that qualitatively this correlation has become quite clear. The details of these investigations can be found in [1,2]

7. Conclusions

The main results obtained by the RD48 collaboration are summarised as follows:

- For charged hadron irradiation the damage induced changes of the effective doping concentration, directly correlating with depletion voltage can be substantially improved by the oxygenation. A hardening effect by a factor of 3 was established for the annealing independent term.
- In addition the reverse annealing amplitude saturates at high fluences, amounting to a reduction factor of up to 3 for DOFZ diodes. The involved time constant is at least larger by a factor of 2. Thus both effects provide a substantial safety margin for the effects to be expected during the warm up maintenance periods.
- Though for MeV neutron irradiation a radiation hardening effect equivalent to that established for charged hadrons is absent, it had been verified that the use of low resistivity silicon is beneficial.
- The Hamburg model for parameterisation of the damage and annealing behaviour is verified also for O-enriched silicon. Simulations for the full 10 years LHC operational scenario have been done both for the ATLAS pixel and microstrip layers. It has been shown that even the pixel sensor for the B-layer, (at $r = 4$ cm), if produced with DOFZ silicon, will withstand the full 10 years LHC operational period.
- The DOFZ technology has proven to be both technologically feasible and cost effective. The transfer to major European detector manufacturers had been successful. Diodes produced this way show superior radiation hardness, fully confirming results which had been obtained by RD48 in earlier tests.
- Up to now the ATLAS pixel and part of the ATLAS SCT group have decided to use the DOFZ technology. Recently also BTeV (at FermiLab) has approved of using the ATLAS pixel design including the DOFZ technique for detector production.

References

[1] RD48 3rd Status Report, CERN/LHCC 2000-009, December 1999.
[2] G. Lindström et al., RD48, Radiation hard silicon detectors—developments by the RD48(ROSE) Collaboration, presented at Fourth STD Hiroshima Conference, March 2000, preprint: ROSE TN/2000/03 see ROSE homepage.
[5] Z. Li et al., IEEE Trans. Nucl. Sci. 39 (6) (1992) 1736.
[6] M. Zielinski et al., Academy of Sciences, Physics Inst. Warsaw, Poland.
[7] M. Wegrzecki, Fourth ROSE Workshop December 1998, CERN/LEB 98-11, p. 133.
[8] B. Sundby Avset et al., SINTEF, 0314 Oslo, Norway.
[9] K. Stolze, CiS Mikrosensorik gGmbH, Erfurt, Germany.
[10] G. Fallica, G. Valvo, STMicroelectronics, Catania, Italy.
[11] C. Wilburn, Micron Semiconductor Limited, UK-Lancing.
[12] M. Moll, Ph.D. Thesis, Hamburg University, 1999, DESY-THESIS-1999-040, ISSN 1435-8085.
[13] M. Moll et al., Nucl. Instr. and Meth. A 426 (1999) 87.
[14] L. Andricek, G. Lutz, Semiconductor Laboratory, MPI Munich, Germany, September 2000, private communication.
[15] G.L.Casse, A comparative study of oxygenated and un-oxygenated Si-diodes, miniature and large area microstrip detectors, Fourth STD Hiroshima Conference, March 2000, see also [3] , p. 164.
[16] A. Ruzin (RD48), Nucl. Instr. and Meth. 447 (2000) 116.
[17] G. Lindström et al., in, p. 184.
[18] J. Wüstenfeld, Ph.D. thesis, University of Dortmund, 2000 see also [3], p. 91 and ROSE/TN/2000-05 in [4].
[19] M. Moll et al., Nucl. Instr. and Meth. 439 (2000) 282 and lit. cited there.
[20] M. Miku et al., Bias Dependence and bistability of radiation defects in silicon, Fourth STD Hiroshima Conference, March 2000.
[21] Z. Li et al., HTLT Oxygenated Silicon Detectors: Radiation Hardness and Long Term Stability, Third International Conference on Radiation Effects on Semiconductor Material, Detectors and Devices, Florence, June 2000.
[22] A. Vasilescu et al., CERN/EP-MIC-SD and INPE Bucharest, June 2000, private communication.
[23] E. Fretwurst et al., Nucl. Instr. and Meth. A 388 (1997) 356.
[24] C. Leroy et al., Nucl. Instr. and Meth. A 426 (1999) 99.
[25] Z. Li et al., in [3], p. 221, see also [21].
[26] T.J. Brodbeck et al., A new method of carrier trapping time measurements, to be publ. In Nucl. Instr. and Meth. A, see also [3], p. 333.
[27] G. Kramberger et al, in [3], p. 353.
[28] E. Fretwurst et al., in [3], p. 315; see also [2].
[29] V. Eremin, Z.Li et al., in [3] p. 374.
[30] G. Lindström, recent analysis of π- and p-induced damage, August 2000, private communication.

[31] R. Wunstorf, August 2000, private communication.
[32] M. Kuhnke, Ph.D. Thesis, Hamburg 2000, see [3], p. 490 and ROSE/TN/2000-04 in [4].
[33] M. Huhtinen, in [3], p. 437.
[34] B. Dezillie et al., The effect of oxygen impurities on radiation hardness of FZ silicon detectors for HEP after n, p and gamma irradiation, in IEEE Trans. Nucl. Sci. (2000), accepted for publication.